PROTEINS
STRUCTURE ■ FUNCTION ■ BIOINFORMATICS

Mechanism of inhibition of wt-dihydrofolate reductase from *E. coli* by tea epigallocatechin-gallate

Michele Spina,[1]* Massimiliano Cuccioloni,[1] Matteo Mozzicafreddo,[1] Francesca Montecchia,[1] Stefania Pucciarelli,[2] Anna Maria Eleuteri,[1] Evandro Fioretti,[1] and Mauro Angeletti[1]

[1] Department of Molecular, Cellular and Animal Biology, University of Camerino, Via Gentile III da Varano, 62032, Camerino (MC), Italy

[2] Department of Comparative Morphological and Biochemical Sciences, University of Camerino, Via Gentile III da Varano, 62032, Camerino (MC), Italy

ABSTRACT

Dihydrofolate reductase (DHFR) is a ubiquitous enzyme involved in major biological process, including DNA synthesis and cancer inhibition, and its modulation is the object of extensive structural, kinetic, and pharmacological studies. In particular, earlier studies showed that green tea catechins are powerful inhibitors of bovine liver and chicken liver DHFR. In this article, we report the results of inhibition kinetics for the enzyme from another source (DHFR from E. coli) exerted by (−)-epigallocatechin-gallate (EGCG). Using different analytical techniques, we reported that EGCG acts as a bisubstrate inhibitor on the bacterial DHFR. Moreover, the combined approach of biosensor, kinetic, and molecular modelling analysis disclosed the ability of EGCG to bind to the enzyme both on substrate (DHF) and cofactor (NADPH) site. Collectively, our data have confirmed the selectivity of antifolate compounds with respect to the different source of enzyme (bacterial or mammalian DHFR) and the possible role of tea catechins as chemopreventive agents.

Proteins 2008; 72:240–251.

Key words: DHFR; EGCG; kinetics; equilibrium study; slow-binding inhibitor; bisubstrate inhibitor.

INTRODUCTION

Dihydrofolate reductase (DHFR—EC 1.5.1.3) is the object of extensive structural and kinetic studies,[1–4] because of its biological and pharmacological relevance. DHFR is an ubiquitous enzyme that catalyzes the reduction of 7,8-dihydrofolate to 5,6,7,8-tetrahydrofolate (THF) using NADPH as cofactor. This enzyme regulates intracellular pools of THF and its derivatives, which are essential cofactors for a number of metabolic pathways in the cell involving the transfer of one-carbon groups. Among such pathways are the biosyntheses of purines and thymidylates (dTMP).[5] In this manner, DHFR plays a key role in DNA replication and cell division, since the enzyme is essential in providing purines and pyrimidine precursors for the biosynthesis of DNA, RNA, and amino acids. Consequently, the inhibition of DHFR, resulting in the disruption of DNA biosynthesis, is the basis of the chemotherapeutic action of a range of DHFR inhibitors, generically referred to as antifolate drugs. Therefore, DHFR is the target enzyme[6] for antifolate drugs such as the antineoplastic drug methotrexate (MTX) and the antibacterial drug trimethoprim (TMP). Because of their structural analogies to MTX, a number of recent studies reported the effects exerted on DHFR by catechins.[7,8]

Catechins belong to a wide family of chemically related polyphenolic compounds, flavonoids, which can be divided into several classes, that is, anthocyanins, flavones, flavonols, flavanones, and so forth. Flavonoid is the general name of compounds based on a 15-carbon skeleton, important secondary metabolites that can be found in plants.[9] In plants, flavonoids can be found in several components, like leaves,[10] seeds,[11] stems, and roots.[12] The main activity of flavonoids is as antioxidants, but they are also involved in physiological regulatory mechanism.[12] Recently, scientific interest has focused on the ways this class of polyphenols act as specific ligands/effectors toward several important macromolecules.[7,13–17] Catechins are a group of polyphenols compounds found in leaves of the green tea *Camelia sinensis*. These compounds represent about 30% of the leaf dry weight. In particular, green tea catechins (GTCs) exhibit marked biological activities[18] and recent studies reported experimental evidences proving that GTCs have potent *in vivo* chemopreventive activity for cancer growth in several experimental models.[19] Recently, a case-control study conducted in

*Correspondence to: Michele Spina, Department of Molecular, Cellular and Animal Biology, University of Camerino, Via Gentile III da Varano, 62032 Camerino (MC), Italy. E-mail: michele.spina@unicam.it
Received 25 April 2007; Revised 20 October 2007; Accepted 6 November 2007
Published online 23 January 2008 in Wiley InterScience (www.interscience.wiley.com). DOI: 10.1002/prot.21914

China showed that green tea consumption is etiologically associated with the incidence of prostate cancer, suggesting the protective effect of green tea against this disease.[20] (−)-epigallocatechin-3-gallate (EGCG) has been the most extensively studied catechin because of its relatively high abundance and strong epidemiologic evidence for *in vitro* and *in vivo* antiproliferative and anticarcinogenic properties.[21,22] Some authors have demonstrated that oral administration of EGCG inhibits carcinogen-induced tumors in various animal.[23]

In a work by Navarro-Perán *et al.*,[8] the author described how (−)-epigallocatechin-3-gallate inhibits the key folate enzyme dihydrofolate reductase (DHFR), and reported the kinetic characteristics of a slow-binding inhibitor exhibited by EGCG against DHFR from bovine liver, and the reversible competitive inhibition against DHFR from chicken liver.

To further understand the nature and the mechanism of this interaction, our work reports a detailed kinetic and equilibrium study on the inhibition of DHFR from *E. coli* by green tea EGCG, taking into account possible disturbing effects, such as the inhibitory effect exerted by folate. Our results suggest that EGCG acts as a bisubstrate inhibitor toward DHFR from *E. coli*. Moreover, the feasible geometry of EGCG-DHFR complexes has been also evaluated using molecular modeling analysis.

MATERIALS AND METHODS

Materials

KH_2PO_4, NaH_2PO_4, KOH, EDTA, NaCl, KCl obtained from J.T. Baker (Netherlands) were of analytical grade. NADPH, ascorbic acid, dihydrofolic acid (DHF), and (−)-epigallocatechin-3-gallate, Tween-20 were obtained from Sigma Aldrich (Milan, Italy). Cellulose acetate filters (0.2 μm) were obtained from Schleicher & Schuell (Dassel, Germany). The carboxylate cuvette and the immobilization kit (NHS, *N*-hydroxysuccinimide; EDC, 1-ethyl-3-(3-dimethylaminopropyl)-carbodiimide; ethanolamine) were obtained from Neosensors Limited (Crewe, UK). Cary-10 UV–vis spectrophotometer was obtained from Varian (Palo Alto, California). Kinetic and thermodynamic studies were performed on an IAsys plus device, Affinity Sensors (Cambridge, UK), obtained from ThermoFinnigan, Italy.

Purification of wt-DHFR

Wild-type DHFR was purified from AG-1 strain of E. coli containing pWT1-3, kindly supplied by Dr. C.R. Matthews (The Pennsylvania State University, Pennsylvania, USA), according to a previously reported procedure.[24] The specific activity of wt-DHFR was 5.5 U mg^{-1} at 20°C and pH 7.0. DHFR samples were stored at 4°C in ammonium sulfate solution. Before each experiment, DHFR was dialyzed overnight against phosphate buffer 50 m*M*, EDTA 0.2 m*M*, pH 7.0. The concentration of DHFR was determined spectrophotometrically at 280 nm using a molar extinction coefficient of 31,100 M^{-1} cm^{-1}.[25]

DHFR assays and kinetic data analysis

The activity of DHFR from *E. coli* was determined at 25°C by following the decrease in the absorbance of NADPH and DHF at 340 nm in a Cary-10 spectrophotometer equipped with 1.0 cm light path cuvettes, thermostatically controlled at 25°C ± 0.5°C.[7,26] Experiments were performed in a buffer containing $K_2(HPO_4)$ 50 m*M*, EDTA 0.02 m*M*, pH 7. To avoid the oxidation of tea catechin, 1 m*M* ascorbic acid was added to the reaction mixture as previously reported.[7] Assays were started by the addition of enzyme. In the absence of the enzyme, the rate of absorbance change was irrelevant. The experimental error associated to the enzymatic activity was determined by calculating the mean value and the standard deviation of replicated assays. To evaluate the possible effects of ascorbic acid on the enzymatic activity, a control activity assay has been performed after addition of wt-DHFR to the buffer solution added with 0.1 m*M* vitamin C. Under these conditions, the reaction initial rate resulted within the calculated experimental error (4.6%). For maximum steady-state rate ($V_{MAX,app}$) and the Michaelis constant for DHF ($K_{m,app}^{DHF}$) determinations NADPH concentration was kept constant at 100 μ*M* and DHF concentration was varied between 5 and 80 μ*M*. Raw data were fitted by nonlinear regression to the integrated form of Michaelis equation for substrate inhibition[27] [Eq. (1)].

$$V = \frac{V_{MAX,app}}{1 + \frac{K_{m,app}^{DHF}}{[S]} + \left(\frac{[S]}{K_i}\right)} \quad (1)$$

Inhibition of dihydrofolate reductase by tea catechin

DHFR (40 n*M*) was incubated at 25°C with increasing concentrations of EGCG in a 50 m*M* phosphate buffer, containing 0.02 m*M* EDTA, 1 m*M* ascorbic acid, pH 7. After 15 min of pre-incubation (longer preincubation times did not yield better inhibition), residual activity were measured at 340 nm by continuously monitoring the disappearance of NADPH and DHF after initiation of the reaction. The residual activity a_i was obtained measuring the initial velocity of the product formation in the absence (V_0) and presence ($V_{0,i}$) of a given flavonoid concentration $[I]_i$:

$$a_i = \frac{V_{0,i}}{V_0} \quad (2)$$

The experimental dataset was constituted by a set of residual activity a_i measured at increasing EGCG concentration $[I]_i$. $K_{m,app}^{DHF}$ and $V_{MAX,app}$ were calculated for each

inhibitor concentration using the Eq. (1). These experiments were repeated at five increasing DHF concentrations (5–80 μ*M*). Each enzymatic activity was repeated in quintuplicate.

Biosensor studies

A carboxylate cuvette was docked into the IAsys Biosensor chamber, washed with PBS-T (NaH_2PO_4 10 m*M*, KCl 2.7 m*M*, NaCl 138 m*M*, Tween-20 0.05%(v/v), pH 7.4), and equilibrated with Tween-free PBS buffer for about 10 min to ensure the establishment of a base line for the sensor trace at the set temperature (30°C). The reaction cell was continuously vibrostirred by a microstirrer installed into the sensing chamber. DHFR was covalently blocked onto the carboxylate matrix of an IAsys biosensor cuvette by a standard EDC/NHS coupling procedure.[28] The non-coupled ligand was removed by washing with PBS buffer for 2 min. Uncoupled carboxygroups were deactivated by a treatment with ethanolamine 1*M*, which also assured the removal of any electrostatically bound material. Finally, the surface was washed and equilibrated with PBS (see Fig. 1). The level of immobilized DHFR was calculated. Readout of about 800 arcsec was obtained. These conditions resulted in the coupling of a 'Langmuir' partial monolayer of about 20 kDa protein (≈1.4 ng/mm^2). A normally distributed population of the immobilized protein in the monolayer was obtained as showed by repeating spot-sampling at different sites (n = 10) on the biosensor surface (data not shown). The cell was equilibrated with 10 m*M* phosphate buffer pH 7 and then the interaction between blocked DHFR and soluble EGCG was investigated by adding increasing concentrations of EGCG (ranging from sub-μ*M* to μ*M*) in presence and in absence of saturating DHF or NADPH. Prior to any further addition of EGCG, dissociation steps were performed by phosphate buffer pH 7 wash, whilst DHFR surface regeneration rate was increased by addition of 10 m*M* CH_3COONa buffer, pH 5.2, being the EGCG-DHFR complex stability reduced in low pH buffers. All association kinetics were followed-up to equilibrium. Binding data were analyzed using the "Fast Fit" software (Fison Applied Sensor Technology), supplied with the instrument; this program uses an iterative curve-fitting to derive the observed rate constant and the maximum response at equilibrium due to ligand binding at a certain ligand concentration [*L*]. The software allows both monoexponential and biexponential models[29,30] to be used to fit experimental data.

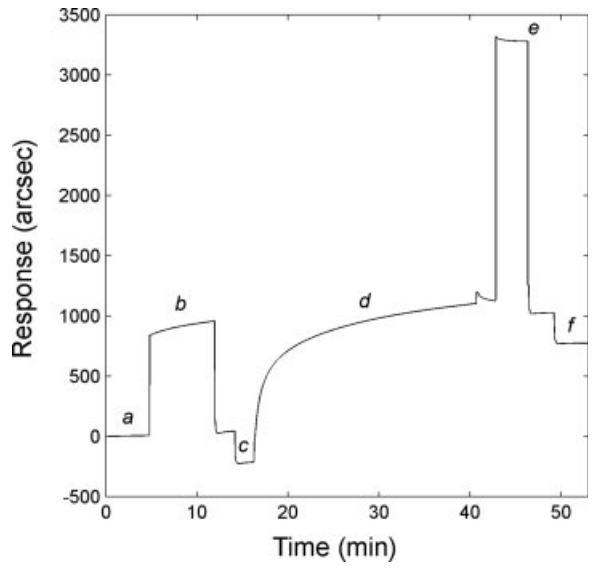

Figure 1

*Immobilization of DHFR to the carboxylate surface. PBS wash and baseline (**a**); surface activation with EDC/NHS (**b**); change to 10 mM acetate buffer pH = 5.2 (**c**); addition of DHFR (**d**); blocking with ethanolamine 1M pH = 8.5 (**e**); wash with 10 mM HCl and PBS (**f**).*

Molecular modeling of the DHFR/EGCG complex

Human DHFR and *E. Coli* DHFR X-ray crystal structures (1S3V[31] and 1RG7[1] pdb entries, respectively) were retrieved from the protein data bank,[32] and hydrogen atoms were added to the DHFR molecules prior to docking procedures. Molecular docking studies were performed on a Pentium 4 Linux Red Hat platform using the Docking and the Discover modules of InsightII software (release 2005, Accelrys, Cambridge, UK). The docking was performed by analogy with crystallographic structures. In particular, 30 rotamers of EGCG molecule were generated and minimized by Discover module using InsightII, and each were positioned in proximity of the binding sites. The starting position at a distance of 10 Å from the binding site was randomly (Box-Muller) chosen each time. The docking procedure was carried out constraining both partners to be rigid, and the enzyme being blocked. The composite DHFR/EGCG models (for EGCG binding to both folate and NADPH sites) were geometry optimized by the mean of Discover module using the consistent valence force field and conjugate gradients algorithm to a root mean square derivative of 0.001 kcal/mol. The intermolecular energy ($E_{Total} = E_{Elect} + E_{VdW}$) was found within Evaluate section of the Docking module.

Rationale

Enzyme kinetic data can be analyzed using an extension of the equilibrium theory of ligand binding linkage[33] to macromolecular systems working at steady state, assuming the reaction involving small ligands dissociation-association very fast compared to the catalytic events.[34–36]

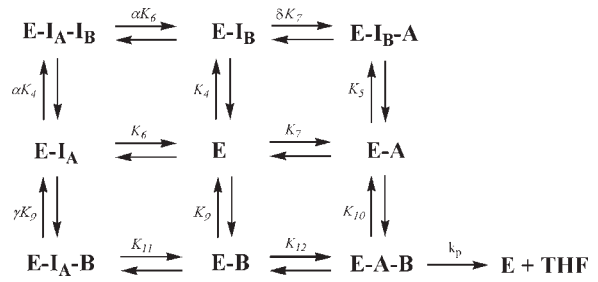

Figure 2

*Possible mechanism for the bisubstrate inhibition of DHFR from E. coli by EGCG (I). We assume the formation of EGCG-DHFR complex both on DHF (E-I$_B$) and NADPH-site (E-I$_A$). The main enzymatic pathway assumes the binding of NADPH (**A**) to free enzyme, followed by the addition of DHF (**B**). The equilibrium are described by the respective dissociation constants.*

We consider a macromolecule E (namely DHFR) having two heterotropically associated binding sites, one for the substrate A (DHF), and one for the substrate B (NADPH).[37] Both sites can each also accommodate a third ligand, the inhibitor I (EGCG), competitively with both substrates. We schematically term the two binding sites (present in the macromolecule E) as site A and site B: the first offering the binding site for NADPH or EGCG, the latter to DHF or EGCG. The macromolecule E exists in nine (differently populated) states. Our model supposes EAB as the only productive complex, as previously reported for DHFR.[38]

The kinetic equation for inhibition of DHFR from *E. Coli* by EGCG, derived from Figure 2, is shown below. This fitting equation was expressed as a function of overall equilibrium dissociation constants, preferred to stepwise reaction parameters, in order to limit the errors associated to cross-correlation between these latter.[39–41]

$$V = \frac{V_{MAX}\frac{[A][B]}{\beta_5}}{1+\frac{[A]}{K_7}+\frac{[B]}{K_9}+\frac{[A][I]}{\beta_2}+\left(\frac{1}{K_4}+\frac{1}{K_6}\right)[I]+\frac{[I]^2}{\beta_3}+\frac{[B][I]}{\beta_4}+\frac{[A][B]}{\beta_5}+\frac{[B]^2}{\beta_i}} \quad (3)$$

Equation 3 can be rearranged in the following Michaelis-like form:

$$V = \frac{V_{MAX,app}}{1+\frac{K_{m,app}^{DHF}}{[S]}+\left(\frac{[S]}{K_i}\right)} \quad (1)$$

with

$$V_{MAX,\,app} = \frac{V_{MAX}\frac{[S_2]}{\beta_5}}{\frac{1}{K_9}+\frac{[I]}{\beta_4}+\frac{[S_2]}{\beta_5}} \quad (4)$$

and

$$K_{m,app}^{DHF} = \frac{1+K_7[A]+\frac{[A][I]}{\beta_2}+\left(\frac{1}{K_4}+\frac{1}{K_6}\right)[I]+\frac{[I]^2}{\beta_3}}{K_9+\frac{[I]}{\beta_4}+\frac{[S_2]}{\beta_5}} \quad (5)$$

The relation between the overall equilibrium dissociation constants and stepwise constants is given by:

$$\beta_2 = K_7K_5 = K_4\delta K_7$$

$$\beta_3 = K_1K_4 = K_6\alpha K_4$$

$$\beta_4 = K_9K_{11} = K_6\gamma K_9$$

$$\beta_5 = K_9K_{12}$$

$$\beta_i = K_iK_9$$

α, δ, γ are nondimensional factors by which ligand equilibrium dissociation constants of the vacant site are shifted upon the binding of another ligand: in fact, on the binding of a ligand (either substrate or inhibitor) to one site, the other site could see its equilibrium constant being shifted (for example, on the binding of I to site A, the site B could see its equilibrium constant being shifted from K_6 to αK_6). Consequently, α, δ, and γ can be considered as a measure of the established conformational coupling upon ligand binding, which is peculiar of DHFR as shown by other authors.[37]

RESULTS

DHFR inhibition by tea EGCG

EGCG strongly inhibited the activity of wt-DHFR from *E. coli*. DHFR activity was continuously assayed after addition of both free and EGCG-preincubated enzyme to assay mixtures containing the two substrates (NADPH and DHF). As previously reported for the inhibition of DHFR from different biological sources by structural folate analogues such as MTX and deazafolates,[42,43] the necessity of preincubation periods suggested a slow establishment of an equilibrium between the enzyme, the inhibitor, and enzyme-inhibitor complex.[42] The hyperbolic dependence of residual activity from the EGCG concentration (see Fig. 3) followed a typical inhibition isotherm. Results reported in Figure 3 showed a slow-binding[44] trend and an incubation-dependent inhibition for EGCG. Since preincubation periods longer than 15 min did not any further affect the time-dependent decreases in reaction rates, all experiments were performed after 15 min preincubation of the EGCG with the protein.

Determination of kinetic parameters of the inhibition

The Michaelis constant (K_m^{DHF}) for the DHFR was experimentally determined by plotting the initial rate V_0 against increasing DHF concentration. Figure 4 shows the Michaelis curves obtained at different EGCG concentrations. These curves showed a substrate inhibition, as early reported,[27] thus raw data were fitted with the

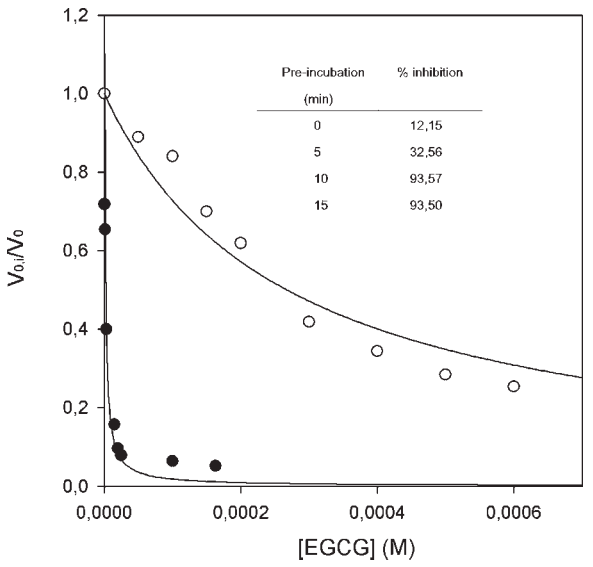

Figure 3

EGCG as "slow-binding inhibitor" of DHFR from E. coli. The normalized initial velocities ($V_{0,i}/V_0$) are plotted as a function of the EGCG concentration. V_0 is the initial velocity in absence of inhibitor. ● EGCG was pre-incubated with DHFR for 15 min. ○ EGCG was not pre-incubated. [DHFR] = 40 nM; [DHF] = 30 mM; [NADPH] = 100 mM. The dependence of DHFR inhibition by 100 μM EGCG upon increasing pre-incubation times is reported in the right inset.

proper equation (see Materials and Methods). $K_{m,app}^{DHF}$, $V_{MAX,app}$ and the catalytic constant k_{cat} for each EGCG concentration were derived from data analysis (see Fig. 5). EGCG acted as a bisubstrate inhibitor[45]: in fact, according to the mechanism presented in Figure 2, it is possible for inhibitor (I) to bind to free enzyme, E-DHF complex (NADPH site) and/or E-NADPH complex (DHF site). Calculated values of $k_{cat}/K_{m,app}^{DHF}$ gave a measure of the catalytic efficiency of the enzymes: data showed in Figure 5 reveals how DHFR has a reduced efficiency at increasing EGCG concentrations.

Biosensor studies—thermodynamics

The binding surface containing immobilized DHFR was obtained as described in Experimental Procedures. The procedure was optimized after several experiments based upon the variation of DHFR concentration and immobilization pH value. A DHFR concentration value of 150 μg/mL and a value of 5.2 for the immobilization pH (chosen on the basis of the DHFR isoelectric point) were found to best suit a good immobilization of DHFR without affecting its functional properties. Under these conditions a final readout of about 800 arcsec, upon DHFR immobilization, was obtained. These data were adequate, since immobilization levels should be fairly low for the particular binding studies analyses, in order to minimize steric hindrance or shielding effects which could affect the analysis. The binding experiment was carried out at increasing EGCG concentrations, each repeated in triplicate. At any titration step, baseline achievement was assessed before adding new EGCG, and then the regeneration steps were achieved as described in Experimental Procedures. Each binding reaction was followed up to equilibrium. In Figure 6, biphasic association and dissociation time-courses of EGCG binding to immobilized DHFR are reported: this behaviour is ascribed to the possible ability of EGCG to bind both folate and NADPH sites. Measured thermodynamic equilibrium constants obtained for this interaction were K_4 = [3.6 ± 0.4] μ*M* and K_6 = [17 ± 6] μ*M*, corresponding to EGCG binding to folate and NADPH sites. As a proof of our assumption, the binding experiments were repeated after saturating DHFR monolayer by addition of NADPH or DHF. In both cases, monophasic time courses were reported, and the equilibrium constant were K_5 = [3.2 ± 0.4] μ*M* and K_{11} = [3.74 ± 0.05] μ*M*, corresponding to EGCG binding to DHF and NADPH site respectively. These results also suggested that EGCG affinity to NADPH site is mildly increased upon DHF binding to DHFR ($K_6 > K_{11}$), being instead EGCG affinity to folate site almost unaffected by NADPH ($K_4 \approx K_5$).

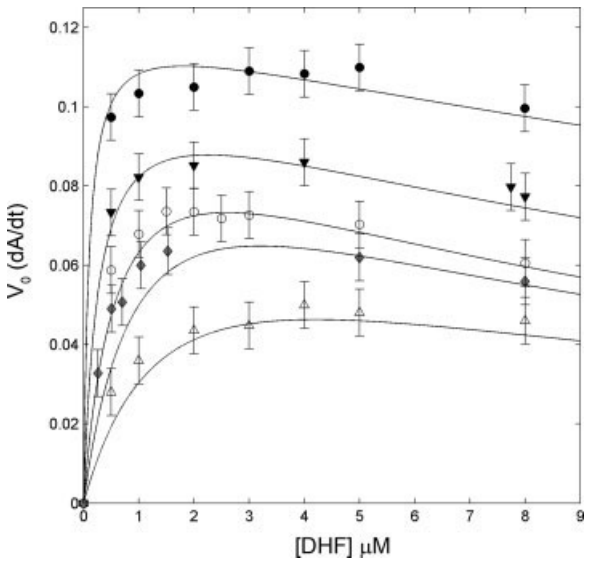

Figure 4

Progress curves for the bisubstrate inhibition of DHFR from E. coli by EGCG. Tea catechin concentration were: (●) 0, (▼) 5, (○) 12.5, (◆) 20 and (Δ) 28.5 μM. The curves and relative standard deviations are global fits of the data to Eq. (1). $K_{m,app}^{DHF}$ and $V_{MAX,}$ for DHFR were obtained by using MatLab 7.3 software. Enzymatic activities were carried out at pH 7.0 and 25.0°C using an enzyme concentration of 40 nM and NADPH concentration of 100 μM. Constant amounts of enzyme were incubated for 15 min with increasing concentrations of EGCG.

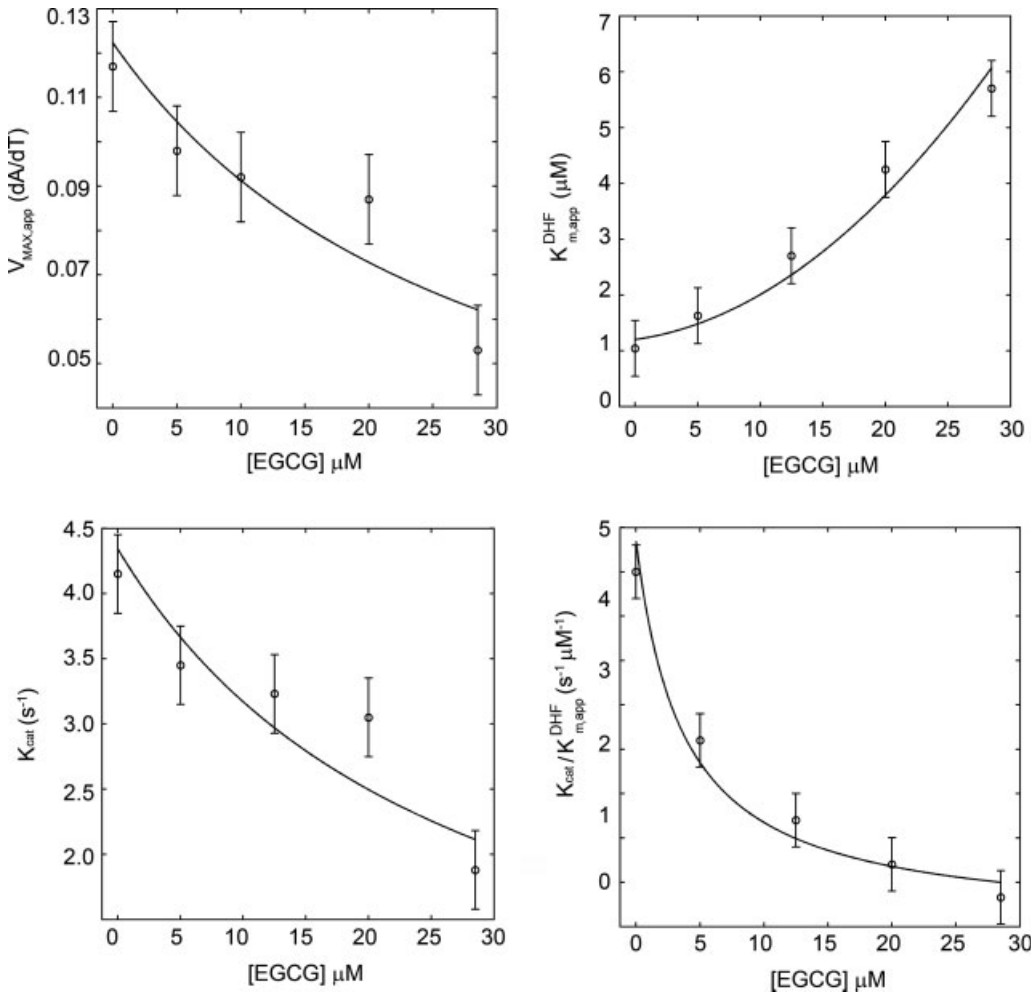

Figure 5

Enzyme kinetic constants for the inhibition of DHFR from E. coli by EGCG. $V_{MAX,app}$, $K^{DHF}_{m,app}$, k_{cat} ($k_{cat} = V_{MAX,app}/[DHFR]_{tot}$) and $k_{cat}/K^{DHF}_{m,app}$ dependence versus tea catechin concentrations were fitted with the proper equations (see Rationale section). The standard deviations to fits are reported.

Biosensor studies—kinetics

The determination of association (k_{ass}) and dissociation (k_{diss}) rate constants for EGCG binding to DHFR unveiled new hidden features of mechanistic properties of their macromolecular recognition process.

With reference to the interaction between the catechin and the free enzyme, preferential EGCG association kinetics to folate site was reported: in fact, EGCG association rate to DHFR at DHF site was about 30 folds higher in comparison with the association at NADPH site. A comparable behavior was reported for dissociation kinetics, being the EGCG dissociation rate from the NADPH site about 6 folds lower. Consequently, the difference in terms of K_D was mainly attributable to association phase.

Moreover, kinetic analysis of EGCG binding to NADPH- or DHF-saturated and free DHFR opened new insights (see Table I) with respect to equilibrium data: in particular, the addition of EGCG to NADPH- and DHF- saturated DHFR results in relevant shift of association rate constants, from 22.50 to 3.4 mM^{-1} s^{-1} for DHF site, and from 0.84 to 2.94 mM^{-1} s^{-1} for NADPH site.

Simultaneously, NADPH saturation induced a shift in k_{diss} value from DHF site from 0.082 to 0.012 s^{-1}. Only minor shift was reported for dissociation rate from NADPH site. Therefore, the kinetic analysis revealed the effect of the saturation with NADPH on the binding of EGCG to DHFR (DHF site), otherwise "thermodynamically-hidden" ($K_4 \approx K_5$).

Molecular modeling of the DHFR/EGCG complex

The docking analysis provided a measure of total intermolecular energy values of the *human* DHFR/EGCG

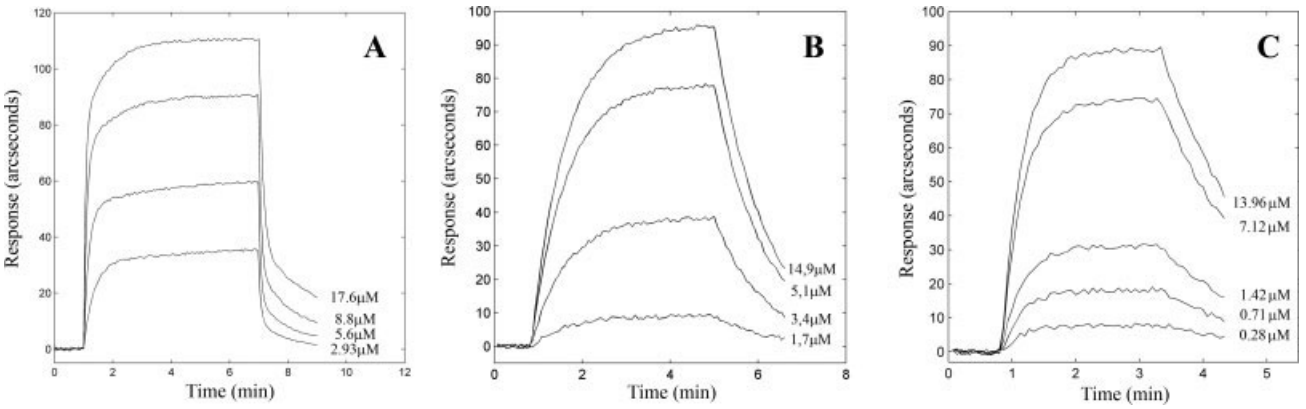

Figure 6

*Binding of EGCG to DHFR (**A**), NADPH-saturated DHFR (**B**) and DHF-saturated DHFR (**C**): overlay of association and dissociation phases measured at increasing concentrations of tea catechin.*

($E_{\text{Tot,humanDHF}} = -82.14$ kcal/mol for the complex at the folate site and $E_{\text{Tot,humanNADPH}} = -69.65$ kcal/mol for the complex at the NADPH site) and *E. coli* DHFR/EGCG complexes ($E_{\text{Tot,EcoliDHF}} = -70.67$ kcal/mol and $E_{\text{Tot,EcoliNADPH}} = -86.02$ kcal/mol). This approach also revealed a mainly electrostatic difference between the *E. Coli* DHFR/EGCG complexes ($E_{\text{Elect.EcoliDHF}} = -16.91$ kcal/mol, ~24% of total energy, and $E_{\text{Elect,EcoliNADPH}} = -40.26$ kcal/mol, ~47% of total energy) and a significative difference in term of Van der Waals energy between the Human DHFR/EGCG complexes ($E_{\text{VdW.humanDHF}} = -60.13$ kcal/mol and $E_{\text{VdW.humanNADPH}} = -44.36$ kcal/mol). In particular, electrostatic energy differences are strongly dependent upon the formation of 7 weak electrostatic H-bonds (mean length = 3.13 Å) in *E. coli* DHFR/EGCG complex at the folate site compared to eight moderate electrostatic H-bonds (mean length = 2.92 Å) in *E. coli* DHFR/EGCG complex at the NADPH site (see Fig. 7). H-bonds of the complex at folate site and at NADPH site are shown in Table II.

DISCUSSION

Recent studies[8] proposing a complete kinetic scheme to explain the slow-binding inhibition of bovine liver DHFR by EGCG show that tea catechins are competitive inhibitors with respect to DHF, preferentially binding to

Table I

*Kinetic and equilibrium dissociation constants for the inhibition of DHFR from **E. coli** by EGCG at 25°C and pH 7.0*

		Kinetic constants	
	Equilibrium constants K (μM)	k_{ass} ($\mu M^{-1}\ s^{-1}$)	k_{diss} (s^{-1})
Binding of EGCG to E-I_B complex[a]	$K_1 = \alpha K6 = 0.024 \pm 0.004$		
Binding of NADPH to E-I_B complex[a]	$K_2 = \delta K_7 = 0.17 \pm 0.03$		
Binding of EGCG to E-I_A complex[a]	$K_3 = \alpha K_4 = 0.006 \pm 0.002$		
Binding of EGCG to DHF-site[b]	$K_4 = 3.6 \pm 0.4$	$k_{ass4} = (22.50 \pm 0.07)*10^{-3}$	$k_{diss4} = 0.082 \pm 0.009$
Binding of EGCG to DHF-site upon NADPH saturation[c]	$K_5 = 3.2 \pm 0.4$	$k_{ass5} = (3.4 \pm 0.2)*10^{-3}$	$k_{diss5} = 0.012 \pm 0.001$
Binding of EGCG to NADPH-site[b]	$K_6 = 17 \pm 6$	$k_{ass6} = (0.84 \pm 0.04)*10^{-3}$	$k_{diss6} = 0.014 \pm 0.005$
Binding of NADPH to free enzyme[d]	$K_7 = 0.17$	$k_{ass} = 20$	$k_{diss} = 3.5$
Binding of DHF to E-I_A complex[a]	$K_8 = \gamma K_9 = 0.098 \pm 0.003$		
Binding of DHF to free enzyme[d]	$K_9 = 0.5$	$k_{ass} = 40$	$k_{diss} = 20$
Binding of DHF to DHFR-NADPH complex[d]	$K_{10} = 1.0$	$k_{ass} = 40$	$k_{diss} = 40$
Binding of EGCG to NADPH site upon DHF saturation[c]	$K_{11} = 3.74 \pm 0.05$	$k_{ass11} = (2.9 \pm 0.02)*10^{-3}$	$k_{diss11} = 0.0109 \pm 0.0001$
Binding of NADPH to DHFR-DHF complex[d]	$K_{12} = 0.34$	$k_{ass} = 5$	$k_{diss} = 1.7$

[a]derived from the overall equilibrium dissociation constants obtained by global fit; standard deviation was calculate by error propagation method.
[b]obtained by fit of biosensor data using a biexponential model[30]
[c]obtained by fit of biosensor data using a monoexponential model[29]
[d]kinetic parameters reported by Howell[38]

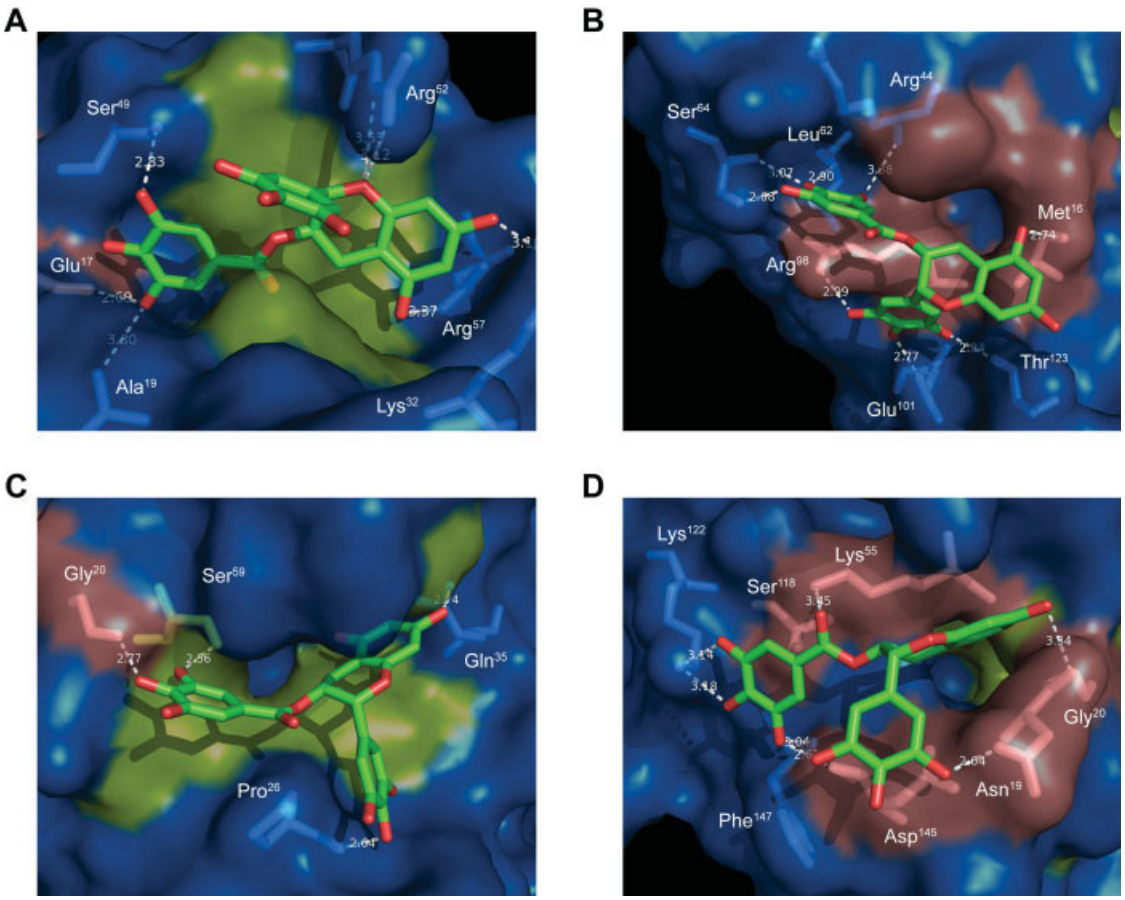

Figure 7

*Molecular docking of the E. coli DHFR/EGCG complexes at the folate site (**A**) and at the NADPH site (**B**), and molecular docking of the human DHFR/EGCG complexes at the folate site (**C**) and at the NADPH site (**D**).*

the free form of the enzyme (K_I = 97.6 n*M*) according to the scheme in Figure 8. These kinetic studies[8] on the inhibition of bovine liver DHFR by tea catechins were performed adding the enzyme to the reaction mixture and simultaneously to both substrates (NADPH and DHF) and the inhibitor. Using a different approach, our kinetic analyses were performed by preincubating the DHFR from *E. coli* with EGCG, and the results have shown an incubation-dependent inhibition, confirming the slow-binding inhibition trend for EGCG, as reported

Table II

H-Bonds Involved in E. coli DHFR/EGCG Complexes

E. coli DHFR/EGCG complex at the folate site	Distance	*E. coli* DHFR/EGCG complex at the NADPH site	Distance	EGCG molecular structure
Glu[17]-O···O (E)	2.69 Å	Met[16]-O···O (H)	2.74 Å	
Ala[19]-N···O (E)	3.30 Å	Arg[44]-N···O (G)	3.38 Å	
Lys[32]-NZ···O (I)	3.10 Å	Leu[62]-O···O (F)	2.90 Å	
Ser[49]-O···O (G)	2.83 Å	Ser[64]-N···O (F)	3.07 Å	
Arg[52]-NE···O (A)	3.53 Å	Ser[64]-OG···O (E)	2.68 Å	
Arg[52]-NH2···O (A)	3.12 Å	Arg[98]-NH1···O (D)	2.99 Å	
Arg[57]-NH1···O (H)	3.37 Å	Glu[101]-OEI···O (C)	2.77 Å	
		Thr[123]-OGI···O (B)	2.84 Å	

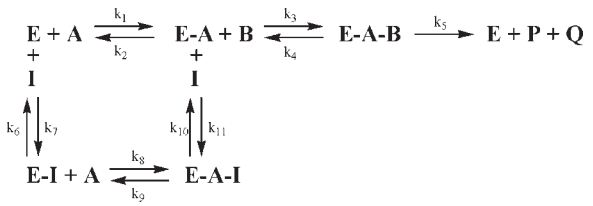

Figure 8

Possible mechanism (proposed by Navarro-Pèran[8]) for the slow-binding inhibition of bovine liver DHFR without pre-incubation of EGCG with enzyme. The mechanism described assumes that the origin of the slow-binding inhibition is the formation of a slowly dissociating complex after the reaction of NADPH with the enzyme-inhibitor complex. The addition of EGCG to EA complex is hindered ($K_I^{EA} \gg K_I^E$). E: free DHFR; A: NADPH; B: DHF; P: $NADP^+$; Q: THF; I: EGCG; $K_I^{EA} = k_{11}/k_{10}$; $K_I^E = k_7/k_6$.

for DHFR purified from a different source.[7,8] The pre-incubation of the enzyme with EGCG has a profound effect on the experimental results: in fact, when the enzyme and inhibitor were pre-incubated for 15 min prior to addition of the substrates, almost complete inhibition of the enzyme was observed, whereas only a limited inhibition was measured when the inhibitor was not pre-incubated with the enzyme.

Using the experimental approach proposed by Navarro-Pèran,[8] we found evidence that EGCG acts as a competitive inhibitor with respect to DHF but not to NADPH.

Differently, preincubating the enzyme with tea catechin, it was possible to further elucidate the inhibition mechanism exerted by EGCG toward DHFR. Kinetic parameters for DHFR from *E. coli* binding to EGCG were determined and the results thus obtained showed that the enzyme, in the presence of tea catechins, may be unable to satisfy cell needs for reduced folates (see Figs. 4 and 5).

Consistently with this, the biosensor data for EGCG revealed a behaviour characteristic of a bisubstrate inhibitor,[45] as recently reported for the inhibition of DHFR from another source by isoniazide.[46] In particular, we obtained evidence suggesting the role of EGCG as a competitive inhibitor with respect to both substrates. In fact, upon saturation of DHFR with DHF or NADPH, monophasic curves for the binding of EGCG to DHFR have been measured, whilst in absence of substrate-saturation, biphasic curves for binding of EGCG to free DHFR were observed. This behaviour suggested clearly the presence of two binding sites for EGCG on DHFR from *E. coli* (see Fig. 6). Furthermore, according to biosensor analysis, the interaction of EGCG with the preformed DHFR-NADPH complex was characterized by an equilibrium dissociation constant of $K_5 = 3.2\ \mu M$: this result suggests that NADPH does not significantly affect EGCG binding to the folate site of DHFR from *E. coli*, unlike the data reported for bovine liver DHFR,[8] where the dissociation constant for the binding of the inhibitor to the DHFR-NADPH complex was ~500-fold higher with respect to the binding of the inhibitor to the free enzyme. Further evidence confirming the selectivity of antifolate compounds with respect to the different sources of enzyme (bacterial or mammalian DHFR),[47–49] was the difference in equilibrium dissociation constants for the binding of tea catechin to DHFR-NADPH complexes, almost 18-fold lower than those reported by Navarro-Pèran.[8] A slightly different behavior was reported for the DHFR-DHF complex: in fact, the equilibrium dissociation constant for the binding of EGCG to the preformed DHFR-DHF complex was five-fold lower in comparison with the one obtained upon binding of EGCG to free enzyme (see Table I).

A model illustrating the mechanism of inhibition of DHFR from *E. coli* by EGCG is proposed in Figure 2 and described in the Rationale section. According to this model and consistent with the biosensor data, EGCG is able to bind DHFR on both site B (substrate site, forming a complex named $E\text{-}I_B$) and site A (cofactor site, forming a complex named $E\text{-}I_A$), prior to the addition of saturating NADPH. Instead, in absence of pre-incubation of the enzyme with tea catechin, NADPH competes with the inhibitor for the same site, and the binding of NADPH ($K_7 = 0.17\ \mu M$) is preferential with respect to EGCG ($K_6 = 17\ \mu M$). In fact, without a pre-incubation step, the affinity of NADPH to the free enzyme is 100-fold higher than EGCG, and there is not a significant binding of the inhibitor to the enzyme on the cofactor-site. A possible mechanism that explains the absence of bisubstrate inhibition of bovine liver DHFR under such conditions is reported in Figure 8. Instead, if the enzyme is preincubated with the inhibitor, the DHFR-EGCG complexes are highly populated, with EGCG binding both on DHF site ($K_4 = 3.6\ \mu M$) and NADPH site ($K_6 = 17\ \mu M$). The kinetic rate constant for the dissociation of inhibitor from the NADPH-site of the enzyme was calculated to be 0.014 s^{-1}, therefore the inhibitor is hardly displaced by NADPH, even possessing this latter higher affinity for its own site; in fact, the displacing is kinetically-controlled as also confirmed by the decrease in k_{cat} upon EGCG addition.

Global fit analysis of kinetic raw data (performed with a two-variables non-linear least-squares data-fitting which uses the Marquardt-Levemberg and Frazier-Suzuki algorithm,[50] developed under MatLab 7.3) allowed the determination of the overall parameters, and the derivation of α, γ, and δ factors, which can be considered an expression of the DHFR heterotropic effect induced by ligand binding. These results could be considered as evidence of the mutual conformational modification of the two binding sites (see Results on Biosensor studies-Kinetics section). In fact, our data proved that the binding of EGCG at the DHF site significantly increased the affinity of the enzyme for a second ligand, either EGCG or NADPH,

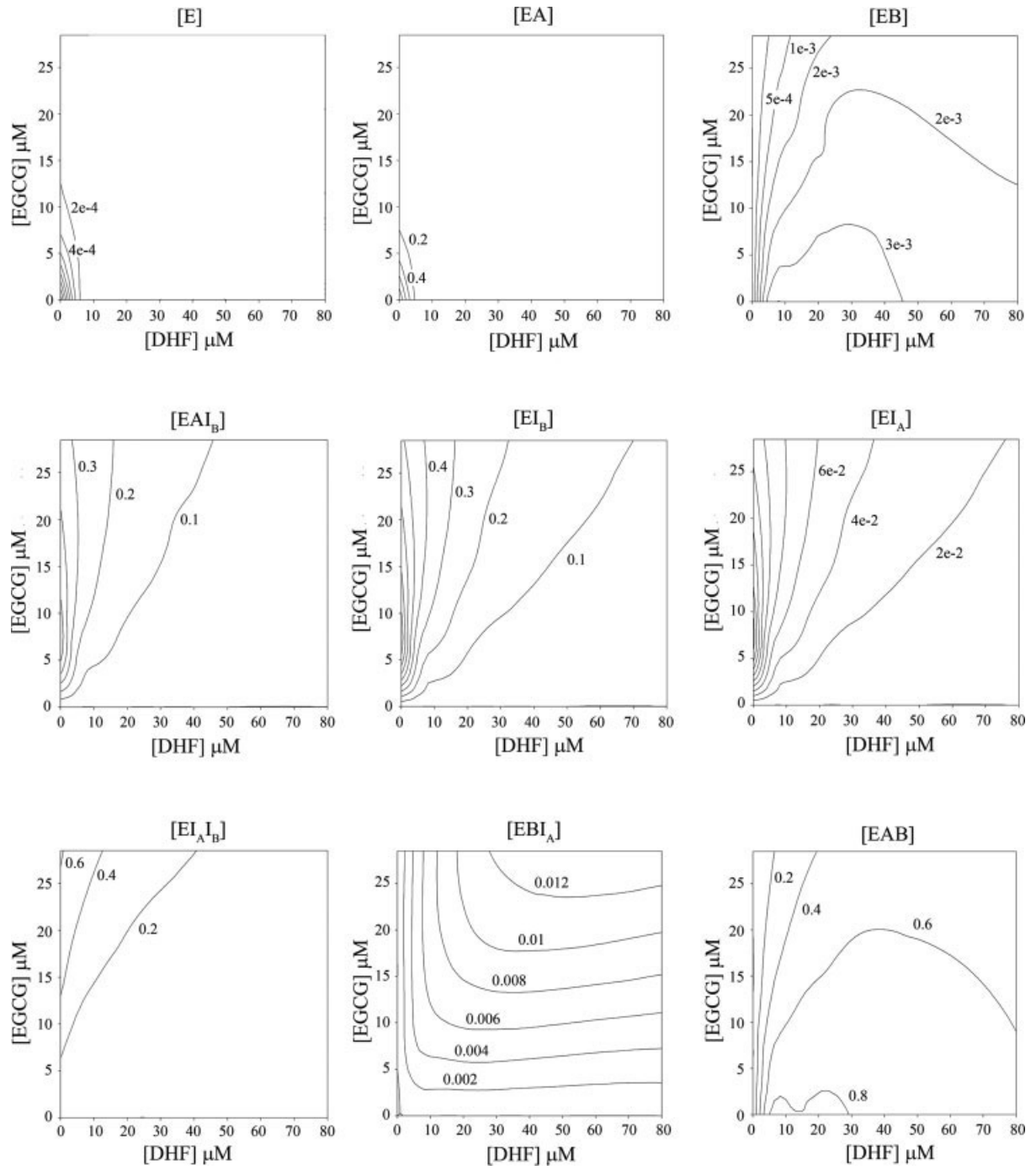

Figure 9

The species fraction of the nine complexes populated at equilibrium as a function of EGCG and DHF concentrations.

with α and δ ≪ 1; the binding of EGCG at the NADPH site had the same significant effect only on the binding of a second molecule of EGCG and a minor effect on the binding of DHF (γ = 0.2).

The scheme in Figure 2 describes the dependence of $V_{MAX,app}$ and $K_{m,app}^{DHF}$ versus EGCG (I) increasing concentrations. In fact, at increasing [*I*] the equilibria will be shifted toward the ternary complex *E*-I_A-I_B, thus populating the *E*-I_B, *E*-I_A-I_B and *E*-I_B-*A* forms, and consequently $K_{m,app}^{DHF} > K_m^{DHF}$ or in other words producing an apparent reduction of the affinity of E for B. Moreover, as long as the inhibitor is present, some of the enzyme will always be

in the nonproductive form such as $E\text{-}I_A\text{-}B$ and $E\text{-}I_B\text{-}A$, even at infinitely high substrates concentrations. Consequently, $V_{MAX,app} < V_{MAX}$. Theoretically, at very high inhibitor concentration ($[I] \gg 600\ \mu M$), all the enzyme can be driven to the $E\text{-}I_A$, $E\text{-}I_B$, $E\text{-}I_A\text{-}B$ and $E\text{-}I_B\text{-}A$ forms, as the velocity is driven to zero. The species fraction of the nine complexes populated at equilibrium (as a function of the EGCG and DHF concentrations) were also calculated[41] (see Fig. 9). Phenomenologically, our system behaves as a mixed-type inhibition[33] as confirmed by analysis of the dependence of the kinetic parameters on EGCG concentration [see Fig. 5 and Eqs. (4) and (5)].

Docking analysis performed on the EGCG-DHFR complex permitted evaluation of the feasible binding geometry of EGCG and DHFR from *E. coli*. Using the DHFR/NADPH and DHFR/DHF complexes as templates, EGCG was docked onto this protein and the resulting complexes were energy minimized. The results account for a promoted binding of the catechin on the NADPH-site of enzymes in terms of total intermolecular energy, in comparison with EGCG-DHFR complex on the DHF-site. This difference is mainly attributable to the electrostatic component, which is about 20% higher in the NADPH-site, in agreement with the lower kinetic dissociation rate for EGCG binding to the NADPH-site (see Table I). As a comparison, docking analysis of human DHFR-EGCG complex was performed. The complexes were characterized by higher stability for EGCG binding to the folate site, and reduced stability for the binding at the NADPH site: this difference could be interpreted as further evidence of a purely competitive inhibition, as reported for EGCG binding for another source of DHFR.[8]

It can be concluded that EGCG exhibits characteristics of a slow binding inhibition against DHFR from *E. coli*, where the enzyme-inhibitor complex is slowly formed (association kinetic rates for the EGCG binding to enzyme are 1000-folds lower than corresponding association rates for substrate and cofactor, respectively), and then undergoes slow dissociation of the inhibitor ($k_{diss4} = 0.082\ s^{-1}$ on the DHF-site, $k_{diss6} = 0.014\ s^{-1}$ on the NADPH-site). Under such conditions, only if DHFR-EGCG complex is added to DHF and saturating NADPH we can observe the binding of inhibitor on the NADPH-site. The crucial step of the kinetic data of the inhibition was the pre-formation of a slowly dissociating complex upon the reaction of EGCG with the enzyme.

In conclusion, in addition to the potential physiological and pathological role exerted by EGCG, the data reported in this study show that DHFRs from bacterial or mammalian sources are all inhibited by EGCG, although through different pathways and mechanisms, the latter fully clarified only by combining different experimental approaches. Collectively, the results presented here confirm the role of tea catechins as possible precursors of potent chemopreventive agents.[8,19]

ACKNOWLEDGMENTS

The authors thank Professor C.R. Matthews (University of Massachusetts Medical School) for kindly providing pWT1-3 and Dr. Carlo Ventura for his technical assistance.

REFERENCES

1. Sawaya MR, Kraut J. Loop and subdomain movements in the mechanism of *Escherichia coli* dihydrofolate reductase: crystallographic evidence. Biochemistry 1997;36:586–603.
2. Miller GP, Benkovic SJ. Strength of an interloop hydrogen bond determines the kinetic pathway in catalysis by *Escherichia coli* dihydrofolate reductase. Biochemistry 1998;37:6336–6342.
3. Sham YY, Ma B, Tsai CJ, Nussinov R. Thermal unfolding molecular dynamics simulation of *Escherichia coli* dihydrofolate reductase: thermal stability of protein domains and unfolding pathway. Proteins 2002;46:308–320.
4. Pucciarelli S, Spina M, Montecchia F, Lupidi G, Eleuteri AM, Fioretti E, Angeletti M. Peroxynitrite-mediated oxidation of the C85S/C152E mutant of dihydrofolate reductase from *Escherichia coli*: functional and structural effects. Arch Biochem Biophys 2005;434:221–231.
5. Miller GP, Benkovic SJ. Stretching exercises—flexibility in dihydrofolate reductase catalysis. Chem Biol 1998;5:R105–R113.
6. Chabner BA, Roberts TG, Jr. Timeline: chemotherapy and the war on cancer. Nat Rev Cancer 2005;5:65–72.
7. Navarro-Peran E, Cabezas-Herrera J, Garcia-Canovas F, Durrant MC, Thorneley RN, Rodriguez-Lopez JN. The antifolate activity of tea catechins. Cancer Res 2005;65:2059–2064.
8. Navarro-Peran E, Cabezas-Herrera J, Hiner AN, Sadunishvili T, Garcia-Canovas F, Rodriguez-Lopez JN. Kinetics of the inhibition of bovine liver dihydrofolate reductase by tea catechins: origin of slow-binding inhibition and pH studies. Biochemistry 2005;44:7512–7525.
9. Manach C, Scalbert A, Morand C, Remesy C, Jimenez L. Polyphenols: food sources and bioavailability. Am J Clin Nutr 2004;79:727–747.
10. Jaakola L, Maatta-Riihinen K, Karenlampi S, Hohtola A. Activation of flavonoid biosynthesis by solar radiation in bilberry (Vaccinium myrtillus L) leaves. Planta 2004;218:721–728.
11. Routaboul JM, Kerhoas L, Debeaujon I, Pourcel L, Caboche M, Einhorn J, Lepiniec L. Flavonoid diversity and biosynthesis in seed of Arabidopsis thaliana. Planta 2006;224:96–107.
12. del Bano MJ, Lorente J, Castillo J, Benavente-Garcia O, Marin MP, Del Rio JA, Ortuno A, Ibarra I. Flavonoid distribution during the development of leaves, flowers, stems, and roots of Rosmarinus officinalis. Postulation of a biosynthetic pathway. J Agric Food Chem 2004;52:4987–4992.
13. Gutzeit HO, Henker Y, Kind B, Franz A. Specific interactions of quercetin and other flavonoids with target proteins are revealed by elicited fluorescence. Biochem Biophys Res Commun 2004;318:490–495.
14. Lee WJ, Shim JY, Zhu BT. Mechanisms for the inhibition of DNA methyltransferases by tea catechins and bioflavonoids. Mol Pharmacol 2005;68:1018–1030.
15. Ermakova S, Choi BY, Choi HS, Kang BS, Bode AM, Dong Z. The intermediate filament protein vimentin is a new target for epigallocatechin gallate. J Biol Chem 2005;280:16882–16890.
16. Mozzicafreddo M, Cuccioloni M, Eleuteri AM, Fioretti E, Angeletti M. Flavonoids inhibit the amidolytic activity of human thrombin. Biochimie 2006;88:1297–1306.
17. Maiti TK, Ghosh KS, Dasgupta S. Interaction of (-)-epigallocatechin-3-gallate with human serum albumin: fluorescence, fourier transform infrared, circular dichroism, and docking studies. Proteins 2006;64:355–362.

18. Zaveri NT. Green tea and its polyphenolic catechins: medicinal uses in cancer and noncancer applications. Life Sci 2006;78:2073–2080.
19. Bettuzzi S, Brausi M, Rizzi F, Castagnetti G, Peracchia G, Corti A. Chemoprevention of human prostate cancer by oral administration of green tea catechins in volunteers with high-grade prostate intraepithelial neoplasia: a preliminary report from a one-year proof-of-principle study. Cancer Res 2006;66:1234–1240.
20. Jian L, Xie LP, Lee AH, Binns CW. Protective effect of green tea against prostate cancer: a case-control study in southeast China. Int J Cancer 2004;108:130–135.
21. Liao S, Kao YH, Hiipakka RA. Green tea: biochemical and biological basis for health benefits. Vitam Horm 2001;62:1–94.
22. Jung YD, Ellis LM. Inhibition of tumour invasion and angiogenesis by epigallocatechin gallate (EGCG), a major component of green tea. Int J Exp Pathol 2001;82:309–316.
23. Katiyar SK, Afaq F, Perez A, Mukhtar H. Green tea polyphenol (-)-epigallocatechin-3-gallate treatment of human skin inhibits ultraviolet radiation-induced oxidative stress. Carcinogenesis 2001;22:287–294.
24. Iwakura M, Jones BE, Luo J, Matthews CR. A strategy for testing the suitability of cysteine replacements in dihydrofolate reductase from Escherichia coli. J Biochem (Tokyo) 1995;117:480–488.
25. Touchette NA, Perry KM, Matthews CR. Folding of dihydrofolate reductase from *Escherichia coli*. Biochemistry 1986;25:5445–5452.
26. Hillcoat BL, Nixon PF, Blakley RL. Effect of substrate decomposition on the spectrophotometric assay of dihydrofolate reductase. Anal Biochem 1967;21:178–189.
27. Nakano T, Spencer HT, Appleman JR, Blakley RL. Critical role of phenylalanine 34 of human dihydrofolate reductase in substrate and inhibitor binding and in catalysis. Biochemistry 1994;33:9945–9952.
28. Davies RJ, Edwards PR, Watts HJ, Lowe CR, Buckle PE, Yeung D, Kinning TM, Pollard-Knight DV. The resonance mirror: A versatile tool for the study of biomolecular interaction. Tech Protein Chem 1994;5:285–292.
29. Hall DR, Winzor DJ. Use of a resonant mirror biosensor to characterize the interaction of carboxypeptidase A with an elicited monoclonal antibody. Anal Biochem 1997;244:152–160.
30. Shi F, Winzor DJ, Jackson CM Temperature dependence of the thrombin-catalyzed proteolysis of prothrombin. Biophys Chem 2004;110:1–13.
31. Cody V, Luft JR, Pangborn W, Gangjee A, Queener SF. Structure determination of tetrahydroquinazoline antifolates in complex with human and Pneumocystis carinii dihydrofolate reductase: correlations between enzyme selectivity and stereochemistry. Acta Crystallogr D Biol Crystallogr 2004;60 (Part 4):646–655.
32. Berman HM, Westbrook J, Feng Z, Gilliland G, Bhat TN, Weissig H, Shindyalov IN, Bourne PE. The Protein Data Bank. Nucleic Acids Res 2000;28:235–242.
33. Segel I. Enzyme kinetics: behavior and analysis of rapid equilibrium and steady-state enzyme systems. New York: Wiley-Interscience; 1975.
34. Di Cera E, De Cristofaro R, Albright DJ, Fenton JW, II. Linkage between proton binding and amidase activity in human alpha-thrombin: effect of ions and temperature. Biochemistry 1991;30:7913–7924.
35. De Cristofaro R, Di Cera E. Effect of protons on the amidase activity of human alpha-thrombin. Analysis in terms of a general linkage scheme. J Mol Biol 1990;216:1077–1085.
36. Vincenzetti S, Angeletti M, Lupidi G, Cambi A, Natalini P, Vita A. Human placenta cytidine deaminase: proton-linked enzyme activity and substrate binding. Biochem Mol Biol Int 1997;42:477–486.
37. Schnell JR, Dyson HJ, Wright PE. Structure, dynamics, and catalytic function of dihydrofolate reductase. Annu Rev Biophys Biomol Struct 2004;33:119–140.
38. Howell EE. Searching sequence space: two different approaches to dihydrofolate reductase catalysis. Chembiochem 2005;6:590–600.
39. Beechem JM. Global analysis of biochemical and biophysical data. Methods Enzymol 1992;210:37–54.
40. Gill SJ, Connelly PR, Di Cera E, Robert CH. Analysis and parameter resolution in highly cooperative systems. Biophys Chem 1988;30:133–141.
41. Wyman JGS. Binding and linkage—functional chemistry of biological macromolecules. Mill Valley, California: University Science Books; 1990.
42. Stone SR, Morrison JF. Mechanism of inhibition of dihydrofolate reductases from bacterial and vertebrate sources by various classes of folate analogues. Biochim Biophys Acta 1986;869:275–285.
43. Williams EA, Morrison JF. Human dihydrofolate reductase: reduction of alternative substrates, pH effects, and inhibition by deazafolates. Biochemistry 1992;31:6801–6811.
44. Morrison JF, Walsh CT. The behavior and significance of slow-binding enzyme inhibitors. Adv Enzymol Relat Areas Mol Biol 1988;61:201–301.
45. Yu M, Magalhaes ML, Cook PF, Blanchard JS. Bisubstrate inhibition: theory and application to *N*-acetyltransferases. Biochemistry 2006;45:14788–14794.
46. Argyrou A, Vetting MW, Aladegbami B, Blanchard JS. Mycobacterium tuberculosis dihydrofolate reductase is a target for isoniazid. Nat Struct Mol Biol 2006;13:408–413.
47. Sasso SP, Gilli RM, Sari JC, Rimet OS, Briand CM. Thermodynamic study of dihydrofolate reductase inhibitor selectivity. Biochim Biophys Acta 1994;1207:74–79.
48. Matthews DA, Bolin JT, Burridge JM, Filman DJ, Volz KW, Kraut J. Dihydrofolate reductase. The stereochemistry of inhibitor selectivity. J Biol Chem 1985;260:392–399.
49. Gschwend DA, Sirawaraporn W, Santi DV, Kuntz ID. Specificity in structure-based drug design: identification of a novel, selective inhibitor of Pneumocystis carinii dihydrofolate reductase. Proteins 1997;29:59–67.
50. Johnson M, Frasier S. Nonlinear least-squares analysis. Methods Enzymol 1985;117:301–342.